

RESEARCH ARTICLE

Clinical Utility of ^{18}F -APN-1607 Tau PET Imaging in Patients with Progressive Supranuclear Palsy

Ling Li, MD,¹ Feng-Tao Liu, MD, PhD,²  Ming Li, PhD,¹ Jia-Ying Lu, MD,¹ Yi-Min Sun, MD, PhD,² Xiaoni Liang, PhD,² Weiqi Bao, MD, PhD,¹ Qi-Si Chen, MD,² Xin-Yi Li, MD,² Xin-Yue Zhou, MD,² Yihui Guan, MD, PhD,¹ Jian-Jun Wu, MD, PhD,² Tzu-Chen Yen, MD, PhD,³ Ming-Kuei Jang, PhD,³ Jian-Feng Luo, PhD,⁴ Jian Wang, MD, PhD,^{2*} Chuantao Zuo, MD, PhD, and ^{1,5*}  the Progressive Supranuclear Palsy Neuroimage Initiative (PSPNI)

¹PET Center, Huashan Hospital, Fudan University, Shanghai, China

²Department of Neurology & National Clinical Research Center for Aging and Medicine, Huashan Hospital, Fudan University, Shanghai, China

³APRINOIA Therapeutics Co., Ltd, Suzhou, China

⁴Department of Biostatistics, School of Public Health, Fudan University, Shanghai, China

⁵Human Phenome Institute, Fudan University, Shanghai, China

ABSTRACT: Background: ^{18}F -APN-1607 is a novel tau PET tracer characterized by high binding affinity for 3- and 4-repeat tau deposits. Whether ^{18}F -APN-1607 PET imaging is clinically useful in PSP remains unclear.

Objectives: The objective of this study was to investigate the clinical utility of ^{18}F -APN-1607 PET in the diagnosis, differential diagnosis, and assessment of disease severity in patients with PSP.

Methods: We enrolled 3 groups consisting of patients with PSP (n = 20), patients with α -synucleinopathies (MSA with predominant parkinsonism, n = 7; PD, n = 10), and age- and sex-matched healthy controls (n = 13). The binding patterns of ^{18}F -APN-1607 in PET/CT imaging were investigated across groups and examined in relation to their utility in the differential diagnosis of PSP versus α -synucleinopathies. Finally, the relationships between clinical severity scores and ^{18}F -APN-1607 uptake were investigated after adjustment for age, sex, and disease duration.

Results: Compared with healthy controls, patients with PSP showed increased ^{18}F -APN-1607 binding in several subcortical regions, including the striatum, putamen, globus pallidus, thalamus, subthalamic nucleus, mid-brain, tegmentum, substantia nigra, pontine base, red nucleus, raphe nuclei, and locus coeruleus. We identified specific regions that were capable of distinguishing PSP from α -synucleinopathies. The severity of PSP was positively correlated with the amount of ^{18}F -APN-1607 uptake in the subthalamic nucleus, midbrain, substantia nigra, red nucleus, pontine base, and raphe nuclei.

Conclusions: ^{18}F -APN-1607 PET imaging holds promise for the diagnosis, differential diagnosis, and assessment of disease severity in patients with PSP. © 2021 International Parkinson and Movement Disorder Society

Key Words: ^{18}F -APN-1607; tau; progressive supranuclear palsy; α -synucleinopathy; positron emission tomography

***Correspondence to:** Prof. Chuantao Zuo, PET Center, Huashan Hospital, Fudan University, 518 East Wuzhong Road, Shanghai 200235, China; E-mail: zuochuantao@fudan.edu.cn or Prof. Jian Wang, Department of Neurology, Huashan Hospital, Fudan University, 12 Middle Wulumuqi Road, Shanghai 200040, China; E-mail: wangjian_hs@fudan.edu.cn

Ling Li, Feng-Tao Liu, and Ming Li contributed equally to this work.

Jian Wang and Chuantao Zuo jointly supervised the work.

Relevant conflicts of interest/financial disclosures: The authors declare that this research was conducted in the absence of any commercial or financial relationships that could be perceived as a potential conflict of interest.

Funding agencies: J.W. received a Project (No. 2016YFC1306504) from the Ministry of Science and Technology of China, funds (Nos.

91949118, 81771372, 81571232) from the National Natural Science Foundation of China, the Shanghai Municipal Science and Technology Major Project (No. 2018SHZDZX01) and support from ZJ Lab. C.Z. received funds (Nos. 81971641, 81671239, and 81361120393) from the National Natural Science Foundation of China, the Shanghai Municipal Science and Technology Major Project (No. 2017SHZDZX01), and Projects (Nos. 19441903500, and 17JC1401600) from the Science and Technology Commission of Shanghai Municipality. F.L. has received funds (No. 81701250) from the National Natural Science Foundation of China.

Received: 21 December 2020; **Revised:** 8 May 2021; **Accepted:** 12 May 2021

Published online in Wiley Online Library (wileyonlinelibrary.com). DOI: 10.1002/mds.28672

Progressive supranuclear palsy (PSP), a rare neurodegenerative disease associated with pathological accumulation of tau protein, is a common atypical parkinsonism clinically characterized by a complex spectrum of motor and behavioral syndromes.^{1,2} Despite recent advances in magnetic resonance (MR) and positron emission tomography/single-photon emission computed tomography (PET/SPECT) imaging, prompt and accurate diagnosis of PSP remains a challenge. Accordingly, patients with PSP may be misdiagnosed as having other parkinsonian disorders, especially in the earliest stages of the disease.³ The most recent diagnostic criteria for PSP maintain that imaging biomarkers, including midbrain atrophy or hypometabolism detected on MRI or ¹⁸F-fluorodeoxyglucose (¹⁸F-FDG) PET and postsynaptic striatal dopaminergic degeneration identified on ¹²³I-iodobenzamide (¹²³I-IBZM) SPECT or ¹⁸F-desmethoxyfallypride (¹⁸F-DMFP) PET, should be regarded as an aid or support in the diagnostic process.³ Although PSP is a tauopathy, the use of tau PET imaging for the diagnosis of PSP is still in its infancy.

Recent years have witnessed a significant increase in the number of PET tracers with binding affinity for tau deposits. Of them, ¹⁸F-AV-1451 has limited clinical usefulness for PSP because of its poor binding capacity in non-AD tauopathies.^{4,5} Another study demonstrated a significant ¹⁸F-THK-5351 uptake in the globus pallidus and midbrain of patients with PSP.⁶ Although this was sufficient to distinguish between cases with PSP and healthy controls,⁶ obvious “off-target” binding to monoamine oxidase B (MAO-B) hampers the clinical application of ¹⁸F-THK-5351 in the diagnosis of PSP.⁷ ¹¹C-pyridinyl-butadienyl-benzothiazole 3 (¹¹C-PBB3) has also been investigated in PSP and has a limited cross-activity to MAO-B^{8,9}; however, its off-target binding represents a significant caveat.¹⁰ Although second-generation tau tracers (eg, ¹⁸F-PI-2620) can distinguish between patients with PSP and healthy controls, their binding patterns are not significantly associated with age, disease duration, or disease severity.¹¹ Interestingly, an ¹⁸F-labeled PBB3 analogue (propranol modification of PBB3, PM-PBB3, termed ¹⁸F-APN-1607 (also known as ¹⁸F-PM-PBB3), holds promise as a useful tracer for in vivo detection of tau aggregates in patients with Alzheimer’s disease (AD) and other non-AD tauopathies.^{12,13} Compared with ¹¹C-PBB3, ¹⁸F-APN-1607 is characterized by a high signal-to-noise ratio and low retention in the venous sinuses.¹² However, information on its clinical utility in the diagnosis, differential diagnosis, and assessment of disease severity in patients with PSP remains limited.

To shed light on this issue, we designed a pilot proof-of-concept investigation in which the binding patterns of ¹⁸F-APN-1607 were examined in PET/CT studies of patients with PSP, patients with α -synucleinopathies, and healthy controls. Subsequently, regional standardized

uptake value ratios (SUVRs) were compared to assess whether ¹⁸F-APN-1607 binding could distinguish between PSP-Richardson’s syndrome (PSP-RS) and PSP-non-RS (ie, other pooled subtypes). Finally, the relationships between clinical severity score and regional measures of ¹⁸F-APN-1607 uptake were investigated after adjustment for age, sex, and disease duration.

Methods

Participants

The study participants were recruited from the Movement Disorders Clinic, Department of Neurology, Huashan Hospital, Fudan University (Shanghai, China). Between May 2019 and August 2020, patients with PSP (n = 20), patients with α -synucleinopathies (multiple system atrophy with predominant parkinsonism [MSA-P], n = 7; Parkinson’s disease [PD], n = 10), and age- and sex-matched healthy controls (HCs, n = 13) were included in the study. PSP was diagnosed and classified into specific subtypes in accordance with the 2017 Movement Disorder Society (MDS) diagnostic criteria.³ The diagnosis of PD and MSA-P followed the widely accepted PD¹⁴ and MSA-P¹⁵ criteria. All healthy controls had a negative history for neurologic and psychiatric disorders. Ethics approval for the study was received from the institutional review board at the Huashan Hospital (approval number 2019–284). The study protocol conforms to national and international regulations and the ethical guidelines set forth by the Helsinki Declaration. All participants provided written informed consent after receiving a detailed explanation of the study procedures.

Clinical Assessment

After recruitment, all participants were referred to a clinical assessment team. Patients were clinically evaluated and underwent imaging procedures after an overnight fast, that is, following an antiparkinsonian medication withdrawal > 12 hours. Disease severity in patients with PSP and α -synucleinopathy was assessed using the Movement Disorders Society Unified Parkinson’s Disease Rating Scale (MDS UPDRS) and the Hoehn and Yahr (H&Y) scale.¹⁶ The PSP rating scale (PSPrs)¹⁷ was also used to evaluate disease severity. Cognitive function was assessed using the Mini-Mental State Examination (MMSE). The study participants underwent ¹⁸F-APN-1607 PET imaging after completion of clinical assessments. All clinical data were reviewed by an expert committee.

Image Acquisition

After completion of clinical assessments, all participants initially underwent anatomical MRI in a 3.0-T horizontal magnet (Discovery MR750; GE Medical Systems, Milwaukee, WI) followed by ¹⁸F-APN-1607 PET. High-resolution

T1-weighted images were acquired using the following parameters: TE, 3.2 milliseconds; TR, 8.2 milliseconds; TI, 450 milliseconds; flip angle, 12° ; acquisition matrix, $256 \times 256 \times 152$; and voxel size, $1 \times 1 \times 1$ mm. ^{18}F -APN-1607 was prepared in the Huashan Hospital PET center by nucleophilic substitution reaction followed by acid hydrolysis carried out on an ^{18}F -multifunction synthesizer (Beijing 127 PET Technology Co. Ltd., Beijing, China).¹⁸ The tosylate precursor used for radio-synthesis was obtained from APRINOIA Therapeutics (Suzhou, China). PET images were acquired in the Huashan Hospital on a Siemens mCT Flow PET/CT scanner (Siemens, Erlangen, Germany) in 3-dimensional (3-D) mode. A low-dose CT transmission scan was performed for attenuation correction. ^{18}F -APN-1607 was administered intravenously (370 MBq), and patients rested comfortably for 90 minutes.¹² ^{18}F -APN-1607 PET imaging was performed over a 20-minute acquisition time (90–110 minutes). Images were subsequently reconstructed using a 3-D ordered-subset expectation maximization algorithm (4 iterations; 24 subsets; Gaussian filter, 2 mm; zoom, 3). Reconstructed images had a matrix size of $256 \times 256 \times 148$ and a voxel size of $2 \times 2 \times 3$ mm³.

Image Processing

All imaging data were transformed for further processing using the MRICron tool (output format: Neuroimaging Informatics Technology Initiative). Individual PET and the corresponding T1-weighted MRI images were thoroughly coregistered using the SPM12 toolbox (<http://www.fil.ion.ucl.ac.uk/spm/software/spm12/>). The transformation matrix for each segmented T1-weighted MRI image was applied to the matched PET image into the Montreal Neurological Institute (MNI) standard space. Subsequently, normalized images were smoothed with a Gaussian kernel at half-maximum with a 6-mm full-width. Cerebellar gray matter was used as the reference region for SUVR calculations. Cortical and subcortical volumes of interest were identified using the Wake Forest University PickAtlas (version 3.0)¹⁹ and included the following regions: frontal cortex, parietal cortex, occipital cortex, temporal cortex, striatum, caudate, putamen, globus pallidus, thalamus, subthalamic nucleus, midbrain, tegmentum, substantia nigra, red nucleus, pontine base, raphe nuclei, locus coeruleus, and dentate nucleus.²⁰ Mean values obtained from both sides were used for the purpose of analysis.

Criteria for Positive Findings on ^{18}F -APN-1607 Tau PET Imaging

The regional SUVR z score was defined as: (single patient's SUVR – mean SUVR observed in healthy controls)/SD of SUVR value observed in healthy controls.

A regional z score ≥ 2 was considered to define positive findings for semiquantitative interpretation at the regional level.¹¹ The presence of at least 1 positive region has been previously considered a criterion for positivity (1-region positivity approach).¹¹ In light of the distribution of positive regions in patients with α -synucleinopathies and healthy controls (Fig. S5), we also adopted more restrictive standards, that is, the presence of at least 2 positive regions of interest on ^{18}F -APN-1607 tau PET imaging (2-region positivity approach).

Statistical Analysis

Data are presented using descriptive statistics. Groups were compared on baseline variables by the Fisher's exact test for categorical data. Normality of continuous variables was investigated using visual histograms and the Kolmogorov–Smirnov test. The homogeneity of variance was assessed with the F test. When data were normally distributed and the variance was heterogeneous, intergroup comparisons of baseline variables were performed using 1-way analysis of variance followed by post hoc Bonferroni's tests in the 4 study groups. In the presence of a skewed distribution, continuous data were analyzed with the Kruskal–Wallis test followed by post hoc tests for pairwise comparisons. As for multiple comparisons of SUVR values, a generalized linear model (GLM) was used to examine intergroup differences after adjustment for age, sex, and disease duration. Analyses were adjusted for multiple comparisons via the Benjamini–Hochberg procedure to control for the false discovery rate. Differences in continuous variables between patients with PSP-RS and PSP-non-RS (pooled) were analyzed with the Student t test. The single-case positivity distributions among different groups were compared using the chi-square test or Fisher's exact test. Areas under the receiver operating characteristic (ROC) curve (AUC) were calculated to assess the diagnostic accuracy of regional ^{18}F -APN-1607 uptake. The regions with high classification accuracy ($\text{AUC} \geq 0.85$, $P < 0.05$) were reported. The criterion for cutoff point selection in the context of ROC curve analysis is the maximum of the Youden's index.²¹ Pearson's correlation coefficient was used to investigate the association between regional ^{18}F -APN-1607 SUVRs and age or disease duration without correcting for multiple comparisons. A GLM was applied to calculate partial correlations between clinical severity score and the extent of ^{18}F -APN-1607 uptake on PET images in patients with PSP after adjustment for age, sex, and disease duration (when available). All analyses were carried out in SPSS (version 20.0; IBM, Armonk, NY), and statistical significance was determined by a 2-tailed $P < 0.05$.

Results

Subject Characteristics

A total of 20 patients with PSP were finally recruited. Although most patients with PSP had classic PSP-RS ($n = 16$), 4 were diagnosed with variant PSP syndromes (PSP-non-RS, pooled). The general characteristics of patients with PSP, MSA-P, and PD and healthy controls are summarized in Table 1. No significant intergroup differences were observed in terms of age and sex. Disease duration, MDS UPDRS-III, and MMSE scores did not differ across groups; conversely, significant differences were observed with respect to the H&Y scores ($P = 0.035$).

Regional ^{18}F -APN-1607 Binding

On visual inspection, most patients with PSP showed obvious ^{18}F -APN-1607 binding in the subcortical nuclei and brain stem. Such elevated bindings in the basal ganglia and midbrain were absent in the majority of patients with α -synucleinopathies (neither MSA-P nor PD). Cortical tracer uptake was uncommon in PSP, being detectable in 3 patients only (Fig. S1). Representative images of ^{18}F -APN-1607 binding in individual regions are shown in Figure 1. In 4 patients with MSA-P, ^{18}F -APN-1607 binding was evident in the putamen, different from the previously mentioned regions in PSP (Fig. S2). Notably, some participants showed obvious plexus binding (Fig. 1).

Compared with healthy controls, quantitative analyses in patients with PSP revealed a significant increase in

terms of regional ^{18}F -APN-1607 binding for the following regions: striatum, putamen, globus pallidus, thalamus, subthalamic nucleus, midbrain, tegmentum, substantia nigra, pontine base, red nucleus, raphe nuclei, and locus coeruleus (Table 2). Compared with patients with PD, those with PSP had a higher tracer binding in the putamen, globus pallidus, subthalamic nucleus, midbrain, tegmentum, substantia nigra, red nucleus, pontine base, raphe nuclei, and locus coeruleus (Table 2). Compared with the MSA-P group, patients with PSP had higher tracer binding in the globus pallidus, subthalamic nucleus, midbrain, tegmentum, substantia nigra, red nucleus, raphe nuclei, and locus coeruleus (Table 2). Compared with healthy controls, there was a significant increase of ^{18}F -APN-1607 uptake in the putamen ($P = 0.003$) and globus pallidus ($P = 0.020$) in patients with MSA-P, but not in those with PD (Fig. S2).

Analysis of Positive Findings on ^{18}F -APN-1607 PET Imaging

We analyzed the presence of positive findings on ^{18}F -APN-1607 tau PET imaging in the 4 study groups using 2 different methods. Using the 2-region positivity approach, 17 of the 20 patients with PSP (85%) and 5 of the 17 patients with α -synucleinopathies (29%) were classified as ^{18}F -APN-1607 tau PET positive at the single-case level (Fig. 2). In the α -synucleinopathies group ($n = 17$), 2 patients with PD (20%) and 3 patients with MSA-P (43%) were ^{18}F -APN-1607 tau PET positive (Fig. 2; Fig. S3). None of the healthy controls was ^{18}F -APN-1607

TABLE 1 General characteristics of the study groups

	PSP	α -Synucleinopathies		HCs	P
		MSA-P	PD		
Number of subjects	20	7	10	13	—
Disease subgroup (number of subjects)	Probable PSP-RS (16) Probable PSP-P (2) Possible PSP-PGF (1) Suggestive of PSP-P (1)	—	—	—	—
Sex (men/women)	13/7	2/5	6/4	8/5	0.438 ^a
Age, years	63.0 \pm 7.4	60.3 \pm 5.1	59.4 \pm 16.3	60.6 \pm 4.2	0.473 ^b
Disease duration, months	45.1 \pm 30.0	25.9 \pm 11.7	29.9 \pm 17.3	—	0.126 ^c
PSP rating scale score	31.6 \pm 16.6	—	—	—	—
MDS UPDRS-III score	34.2 \pm 15.1	44.0 \pm 8.2	38.9 \pm 17.1	—	0.306 ^c
Hoehn & Yahr scale score	3 (3, 3)	4 (3, 4)	4 (3, 4)	—	0.035 ^b
MMSE	24.1 \pm 4.6	23.9 \pm 4.9	25.4 \pm 4.3	26.7 \pm 2.5	0.337 ^b

^aFisher's exact test.

^bKruskal-Wallis test.

^cOne-way analysis of variance followed by Bonferroni's post hoc correction for multiple comparisons.

PSP-RS, progressive supranuclear palsy-Richardson's syndrome; PSP-P, progressive supranuclear palsy with predominant parkinsonism; PSP-PGF, progressive supranuclear palsy with predominant gait freezing; PSP-P, progressive supranuclear palsy with predominant parkinsonism; MSA-P, multiple system atrophy with predominant parkinsonism; PD, Parkinson's disease; HCs, healthy controls; MDS-UPDRS, Movement Disorders Society Unified Parkinson's Disease Rating Scale; MMSE, Mini-Mental State Examination.

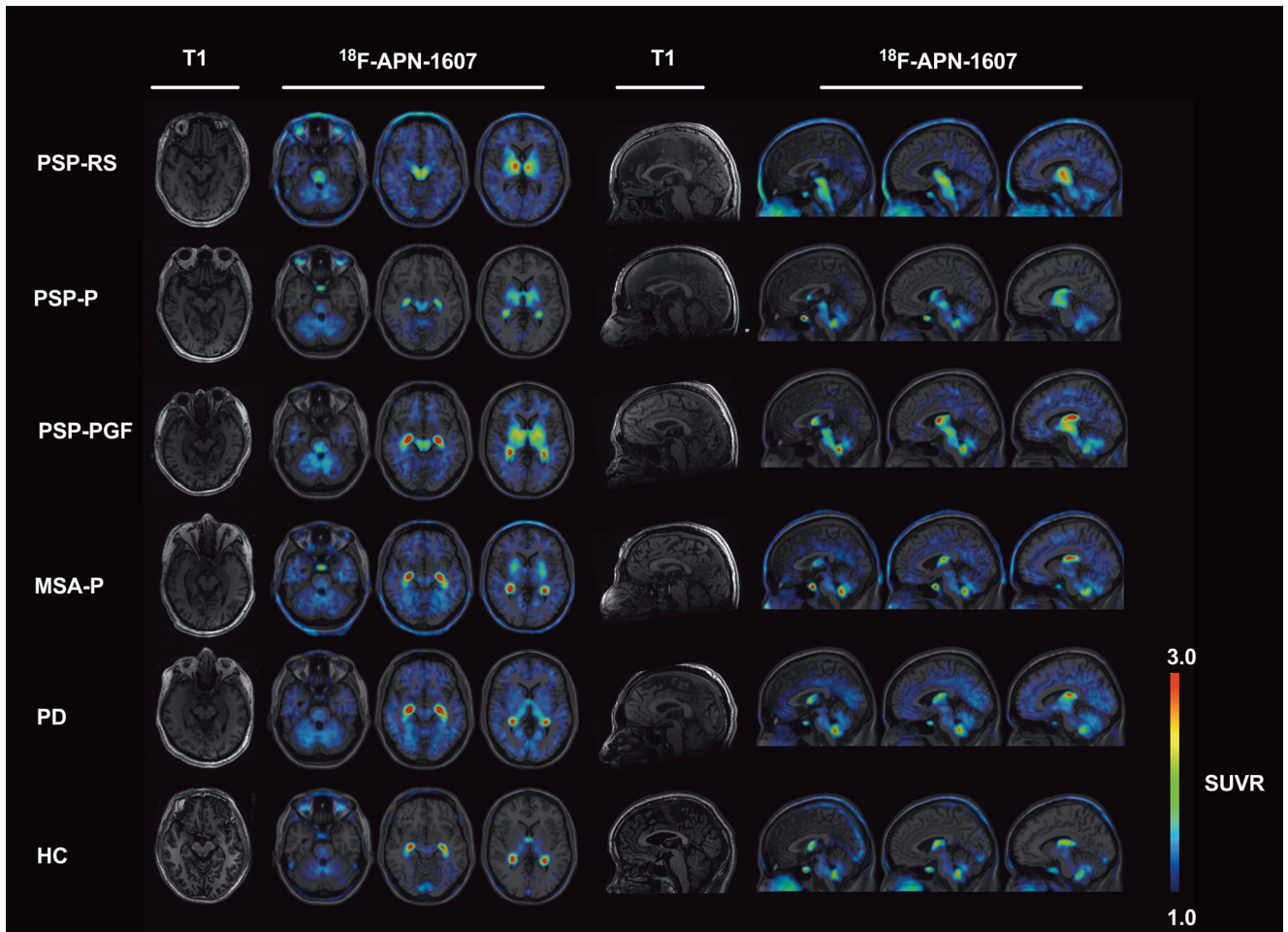


FIG. 1. Representative ¹⁸F-APN-1607 PET images in different groups. Representative individual ¹⁸F-APN-1607 PET images were superimposed to anatomical T1 MRI in patients with PSP, people with α -synucleinopathies, and HCs. Obvious ¹⁸F-APN-1607 bindings in the midbrain and basal ganglia were identified in different PSP subtypes. No prominent tracer binding in the subcortical nuclei and brain stem was observed in patients with α -synucleinopathies (PD and MSA-P). The presence of plexus binding was also evident in different groups. The color stripe indicates the standard uptake value ratio using the cerebellar cortex as the reference region. PSP-RS, progressive supranuclear palsy-Richardson’s syndrome; PSP-P, progressive supranuclear palsy with predominant parkinsonism; PSP-PGF, progressive supranuclear palsy with predominant gait freezing; MSA-P, multiple system atrophy with predominant parkinsonism; PD, Parkinson’s disease; HC, healthy controls. [Color figure can be viewed at wileyonlinelibrary.com]

tau PET positive (Fig. 2A; Fig. S4). The 2-region positivity approach was able to distinguish PSP from healthy controls with a sensitivity of 85% and a specificity of 100%. On analyzing its ability to distinguish PSP from patients with α -synucleinopathies, the sensitivity was 85%, and the specificity was 71% (Table S1). As previously reported,¹¹ the 1-region positivity approach distinguished patients with PSP from healthy controls with a sensitivity of 90% and a specificity of 92%. However, lower specificity (53%) was observed on analyzing its ability to distinguish PSP from patients with α -synucleinopathies (Table S1; Fig. S5). Therefore, our main analysis was based on the 2-region positivity approach (Fig. 2A).

Diagnostic Accuracy of ¹⁸F-APN-1607 Tau PET Findings

ROC curve analysis revealed that SUVRs of most subcortical regions allowed making a reliable differential

diagnosis between PSP and α -synucleinopathies. This was especially evident for SUVRs of the subthalamic nucleus (AUC, 0.935). Using an optimal cutoff value of 1.535 for SUVRs of subthalamic nucleus, ¹⁸F-APN-1607 PET imaging had 95% sensitivity and 82% specificity for distinguishing PSP from α -synucleinopathies. In addition, SUVRs of raphe nuclei, red nucleus, tegmentum, and midbrain were found to distinguish PSP from α -synucleinopathies with high accuracy (Fig. 2B). The differential ability of regional SUVRs in distinguishing PSP from MSA-P, PD, and HC is summarized in Table S2.

Associations between ¹⁸F-APN-1607 Binding and Disease Severity in Different PSP Subtypes

As shown in the heat map of individual ¹⁸F-APN-1607 binding, the subgroup of patients with the PSP-non-RS (pooled) subtype showed a trend toward a low

TABLE 2 Quantitative results (standardized uptake value ratios) of ¹⁸F-APN-1607 binding in different brain regions among the 4 study groups

Brain region	PSP	MSA-P	PD	HCs	PSP vs MSA-P	PSP vs PDP	PSP vs HCP
Frontal cortex	0.95 ± 0.13	0.93 ± 0.05	0.90 ± 0.07	0.93 ± 0.09	0.707	0.354	0.961
Parietal cortex	0.98 ± 0.13	0.96 ± 0.05	0.94 ± 0.12	0.95 ± 0.08	0.788	0.523	0.707
Occipital cortex	1.09 ± 0.12	1.06 ± 0.04	1.06 ± 0.09	1.06 ± 0.09	0.607	0.556	0.707
Temporal cortex	1.06 ± 0.15	1.05 ± 0.07	1.00 ± 0.11	1.02 ± 0.08	0.918	0.380	0.752
Striatum	1.18 ± 0.17	1.15 ± 0.15	1.09 ± 0.10	1.04 ± 0.12	0.788	0.173	0.020 ^a
Caudate	0.92 ± 0.15	0.92 ± 0.15	0.92 ± 0.17	0.92 ± 0.10	0.961	0.961	0.961
Putamen	1.37 ± 0.20	1.36 ± 0.16	1.22 ± 0.09	1.15 ± 0.14	0.961	0.044 ^b	0.003 ^a
Globus pallidus	1.67 ± 0.25	1.43 ± 0.15	1.33 ± 0.13	1.26 ± 0.16	0.036 ^b	<0.001 ^b	<0.001 ^a
Thalamus	1.69 ± 0.29	1.61 ± 0.09	1.47 ± 0.18	1.46 ± 0.16	0.707	0.059	0.038 ^a
Subthalamic nucleus	1.89 ± 0.30	1.42 ± 0.10	1.40 ± 0.29	1.37 ± 0.17	0.001 ^b	<0.001 ^b	<0.001 ^a
Midbrain	1.56 ± 0.23	1.32 ± 0.09	1.29 ± 0.11	1.28 ± 0.15	0.008 ^b	<0.001 ^b	<0.001 ^a
Tegmentum	1.82 ± 0.33	1.40 ± 0.10	1.42 ± 0.12	1.37 ± 0.14	0.001 ^b	<0.001 ^b	<0.001 ^a
Substantia nigra	1.53 ± 0.20	1.35 ± 0.09	1.28 ± 0.16	1.28 ± 0.16	0.042 ^b	0.001 ^b	0.001 ^a
Red nucleus	1.88 ± 0.36	1.41 ± 0.10	1.46 ± 0.13	1.40 ± 0.14	<0.001 ^b	<0.001 ^b	<0.001 ^a
Pontine base	1.39 ± 0.18	1.28 ± 0.09	1.20 ± 0.12	1.22 ± 0.17	0.165	0.002 ^b	0.014 ^a
Raphe nuclei	1.81 ± 0.29	1.35 ± 0.12	1.39 ± 0.14	1.32 ± 0.13	<0.001 ^b	<0.001 ^b	<0.001 ^a
Locus coeruleus	1.50 ± 0.22	1.31 ± 0.12	1.32 ± 0.10	1.25 ± 0.14	0.031 ^b	0.011 ^b	<0.001 ^a
Dentate nucleus	1.46 ± 0.23	1.54 ± 0.21	1.32 ± 0.15	1.36 ± 0.16	0.354	0.215	0.406

^aStatistically significant after adjustment for age and sex and application of the post hoc correction for multiple comparisons.

^bStatistically significant after adjustment for age, sex, and disease duration and application of the post hoc correction for multiple comparisons.

P values from pairwise comparisons of the study groups were adjusted for multiple comparisons via the Benjamini-Hochberg procedure to control for the false discovery rate (FDR) after adjustment for age, sex, and disease duration. PSP, progressive supranuclear palsy; MSA-P, multiple system atrophy with predominant parkinsonism; PD, Parkinson's disease; HCs, healthy controls.

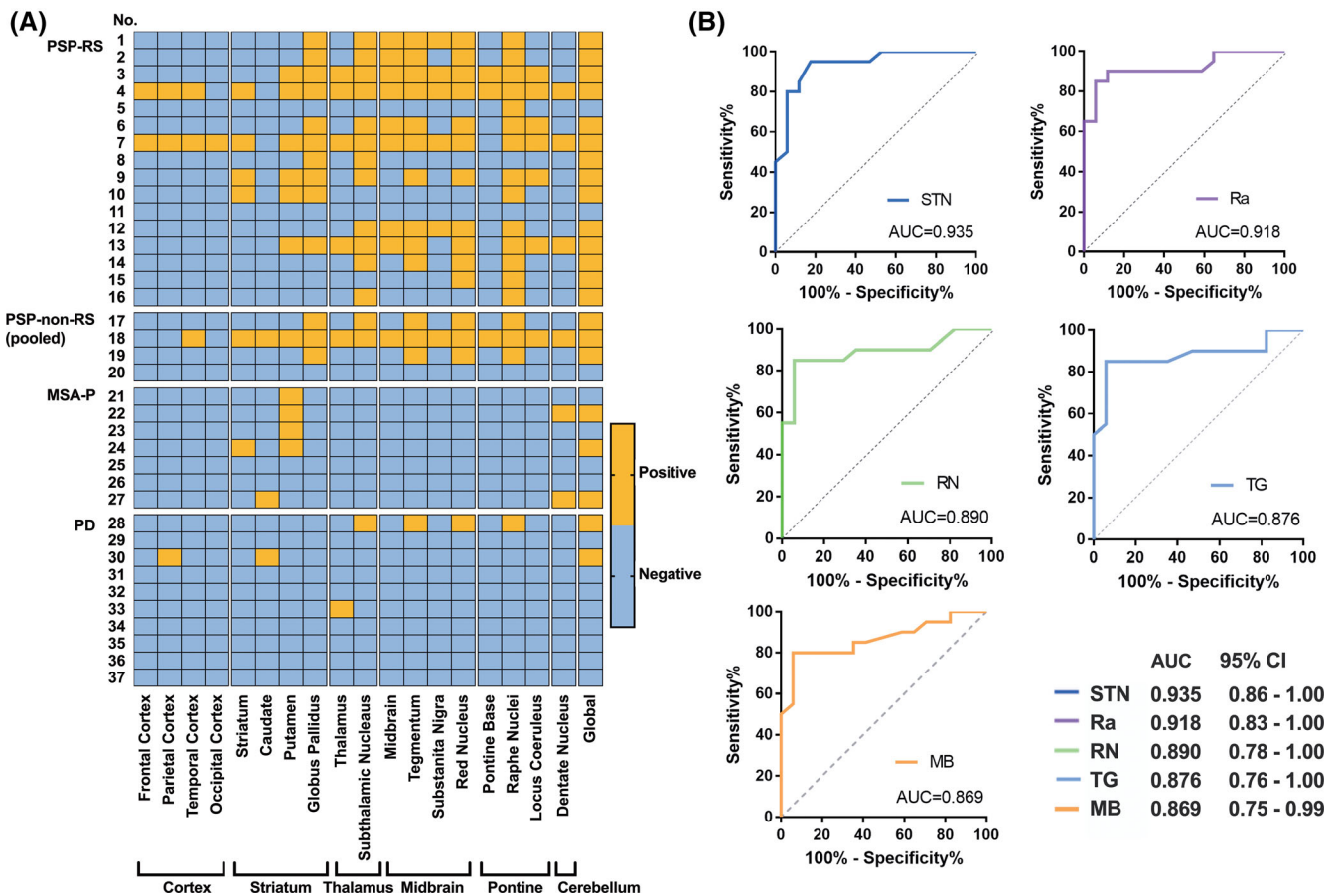


FIG. 2. Clinical utility of ¹⁸F-APN-1607 tau PET imaging in the differential diagnosis of PSP. Clinical utility of ¹⁸F-APN-1607 tau PET imaging in distinguishing PSP from α -synucleinopathies using global PET tau results — positive versus negative (A) and receiver operating characteristic curve analysis of regional SUVRs (B). (A) Individual ¹⁸F-APN-1607 tau PET imaging findings (positive versus negative) in different patient groups. (B) Receiver operating characteristic curves illustrating the diagnostic accuracy of ¹⁸F-APN-1607 binding in different brain regions for the differential diagnosis of PSP versus α -synucleinopathies. The accuracy of the model was assessed by calculating the areas under the receiver operating characteristic curves. PSP, progressive supranuclear palsy; MSA-P, multiple system atrophy with predominant parkinsonism; STN, subthalamic nucleus; Ra, raphe nuclei; RN, red nucleus; TG, tegmentum; MB, midbrain. [Color figure can be viewed at wileyonlinelibrary.com]

tracer uptake (Fig. 3A). Similarly, they tended to have lower *z* scores (both total score and at the regional level) – albeit not significantly so (Fig. 3B). The associations between the severity of PSP (as assessed by PSPrs scores) and the extent of ¹⁸F-APN-1607 uptake (as expressed by SUVRs) were analyzed separately for different ROIs without applying a correction for multiple comparisons. The SUVR of subthalamic nucleus (*P* = 0.035), midbrain (*P* = 0.014), substantia nigra (*P* = 0.030), red nucleus (*P* = 0.014), pontine base (*P* = 0.043), and raphe nuclei (*P* = 0.005) showed positive correlations with PSPrs scores after adjustment for age, sex, and disease duration (Fig. 3C). Notably, neither age nor disease duration was found to correlate with ¹⁸F-APN-1607 uptake (Table S3).

Discussion

In the current study, we provide initial proof-of-concept evidence that ¹⁸F-APN-1607 PET imaging may

serve as an imaging tool for distinguishing PSP from α -synucleinopathies (MSA-P and PD). Although cases with PSP showed a clear ¹⁸F-APN-1607 binding in the basal ganglia and midbrain, such binding patterns were rare in patients with α -synucleinopathies or healthy controls. However, 4 cases with MSA-P showed clear ¹⁸F-APN-1607 binding in the basal ganglia, but not in the midbrain. Moreover, we found that the severity of PSP was positively correlated with SUVRs measured in certain ¹⁸F-APN-1607-positive regions. Pending independent validation, our pilot observations suggest that ¹⁸F-APN-1607 PET may serve as a promising imaging biomarker for the diagnosis, differential diagnosis, and assessment of disease severity in patients with PSP.

On identifying areas of increased ¹⁸F-APN-1607 uptake in patients with PSP (striatum, putamen, globus pallidus, thalamus, subthalamic nucleus, midbrain, tegmentum, pontine base, substantia nigra, red nucleus, raphe nuclei, and locus coeruleus), we confirmed that their distribution was consistent with the typical tau spreading pattern in PSP pathology.²² First-generation

tau tracers have shown either low affinity or limited signals for non-AD tauopathies,^{23,24} being ultimately limited for the imaging of patients with PSP. Recent studies have focused on the potential utility of second-generation tau PET tracers, including ¹⁸F-PI-2620¹¹ and ¹⁸F-APN-1607,¹² in this clinical entity (Table S4). Studies conducted using first-generation tracers have been partially limited by the occurrence of off-target binding in the basal ganglia, midbrain, thalamus, choroid plexus, and venous sinus.²⁴ Specifically, ¹⁸F-THK5351 showed off-target binding to MAO-B,²⁵ whereas ¹⁸F-AV-1451 signals tended not only to increase with age but also displayed off-target activity because of neuromelanin and brain hemorrhagic lesions.²⁶ Notably, ¹⁸F-APN-1607 uptake did not correlate with age in either disease groups (regardless of a diagnosis of PSP or α -synucleinopathies) or in healthy controls. Although these results suggest that off-target activity from brain aging was unlikely, caution should be exercised on the occurrence of off-target binding because background activity was elevated and plexus binding was observed.

Once we had obtained initial evidence indicating that ¹⁸F-APN-1607 binding could be increased in subcortical areas of patients with PSP, we then included it in the imaging protocol patients with α -synucleinopathies. This allowed us to demonstrate the usefulness of ¹⁸F-APN-1607 PET for a differential diagnosis. In our study, the ¹⁸F-APN-1607 binding patterns of patients with PSP were obviously different from those observed in α -synucleinopathies. Interestingly, 4 cases with MSA-P in our study had increased ¹⁸F-APN-1607 binding in the putamen. This has been shown to result in low specificity when the 1-region positivity approach was used to distinguish PSP from α -synucleinopathies.¹¹ A previous investigation demonstrated asymmetric ¹⁸F-AV-1451 uptake in the putamen of patients with MSA-P, which may be at least in part attributable to off-target binding.²⁷ However, we identified ¹⁸F-APN-1607 binding in the putamen of patients with MSA-P (4 of 7), but not of those with PD. These results can be explained either by the presence of tau deposits in the putamen²⁸ of the former patient group or by off-target binding of the tracer to other proteins not limited to

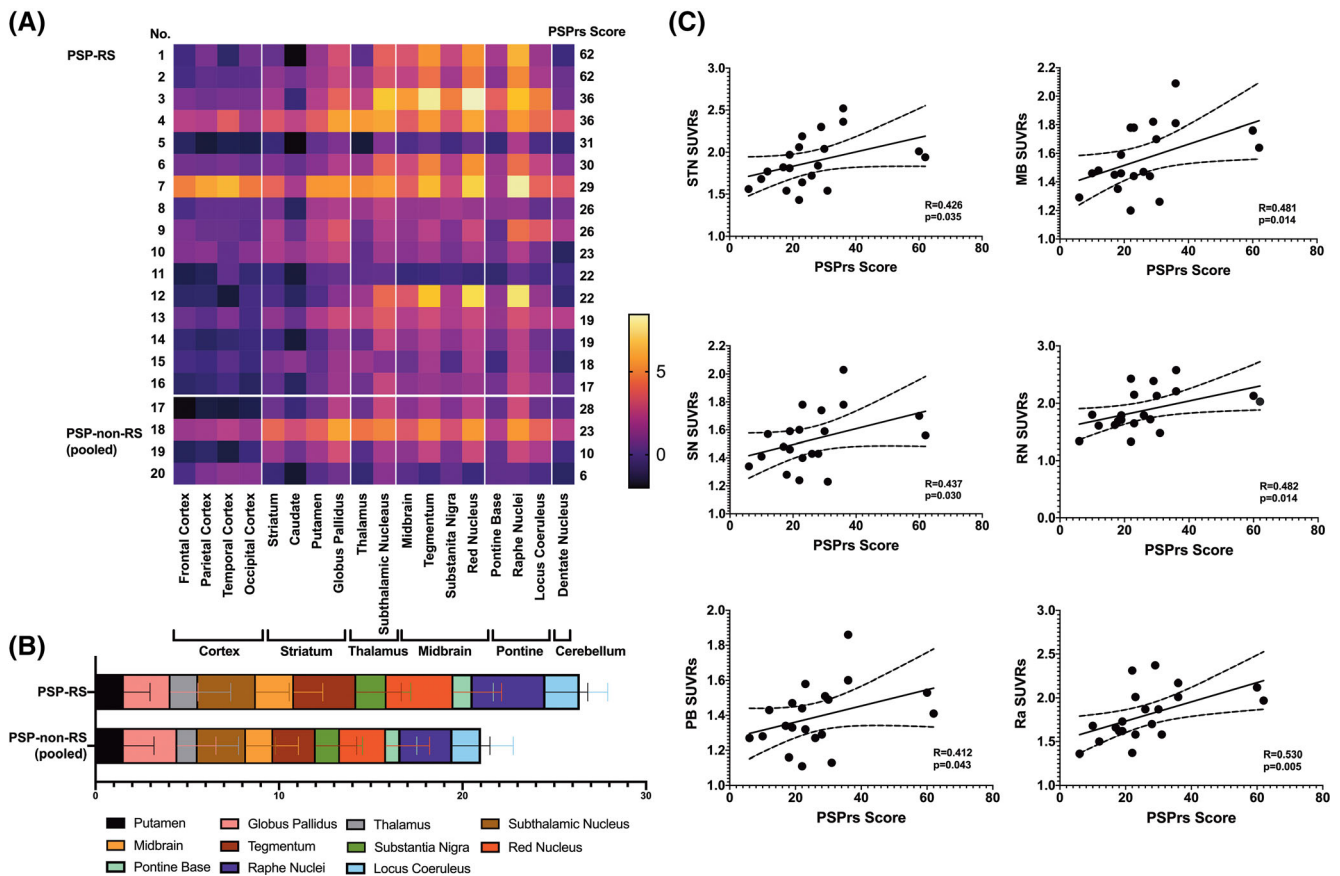


FIG. 3. ¹⁸F-APN-1607 uptake and clinical severity of PSP. Heat map of regional z scores at the patient level (A) and summed vectors of regional z scores in different PSP phenotypes (B) identified a trend toward increased tau deposition in PSP-RS. (C) Partial correlation analyses in patients with PSP revealed significant positive associations between regional ¹⁸F-APN-1607 bindings and disease severity (as assessed by PSPrs scores) after adjustment for age, sex, and disease duration using a generalized linear model. PSP-RS, progressive supranuclear palsy–Richardson’s syndrome; STN, subthalamic nucleus; MB, midbrain; SN, substantia nigra; RN, red nucleus; PB, pontine base; Ra, raphe nuclei; PSPrs, progressive supranuclear palsy rating scale. [Color figure can be viewed at wileyonlinelibrary.com]

MSA-related α -synuclein.²⁹ Future studies should examine in greater detail the clinical utility of ¹⁸F-APN-1607 PET imaging in patients with MSA-P.

PSP includes different disease subtypes that have distinct clinical courses and tau accumulation patterns. Our study is the first to analyze SUVRs from ¹⁸F-APN-1607 PET in relation to different PSP variants. In agreement with the results from a pathology study,²⁰ we found a trend toward increased tau accumulation (as reflected by ¹⁸F-APN-1607 binding) in patients with the PSP-RS than in those with PSP-non-RS (pooled). There were 3 cases in the PSP cohort with negative tau PET imaging (Fig. 2; Fig. S3). Although the definition of standard positive uptake ($Z \geq 2$) may be too strict for some patients with PSP, it is possible that the burden of tau accumulation at the time of examination was below the detection threshold. A thorough follow-up will be necessary to confirm the diagnosis in the presence of clinical symptoms and negative ¹⁸F-APN-1607 PET imaging findings.

Another interesting observation in our study is the positive association between PSP severity and SUVRs measured in several subcortical regions (ie, subthalamic nucleus, midbrain, substantia nigra, red nucleus, pontine base, and raphe nuclei). Owing to the exploratory nature of the study and the limited sample size, we did not apply a post hoc correction for multiple comparisons when correlation analyses based on different ROIs were undertaken. Notably, this is consistent with the previous finding of a significant correlation between ¹⁸F-APN-1607 SUVRs in the subthalamic nucleus and PSPrs scores.¹² Pathologic alterations in the subthalamic nucleus are common in PSP.³⁰ The increased signal observed in these nuclei may be attributable to the prion-like propagation of tau fibrillogenesis,²⁰ which may play a role in disease progression. Although our findings should be considered as hypothesis generating, the clinical utility of ¹⁸F-APN-1607 PET imaging for the diagnosis, differential diagnosis, and assessment of disease severity in PSP warrants further scrutiny.

Our study has 2 main strengths. First, our research was not limited to patients with PSP and healthy controls. The inclusion of cases with α -synucleinopathies allowed us to assess whether ¹⁸F-APN-1607 PET imaging has value for differential diagnosis. Second, the selection of the regions of interest for this study, including the cortex, striatum, thalamus, brain stem, and cerebellum, was informed by recent pathological studies.²⁰ Our investigation also has some limitations. First, patients with PD had severe symptoms despite short disease duration. This can be explained by the small sample size and/or that patients with severe disease despite short disease duration are more likely to be included in PET imaging studies, potentially implying a selection bias. Future studies with larger samples should work to address this caveat. A higher number of

patients may also provide greater power to evaluate whether differences in terms of ¹⁸F-APN-1607 binding exist between different PSP subtypes. Second, we relied on a nondynamic acquisition protocol. In an effort to minimize the impact of blood flow, we adopted the methodological approach described by Tagai et al.¹² Third, we did not perform visual interpretation of PET images.

Conclusion

Our pilot results suggest that ¹⁸F-APN-1607 PET imaging has the potential for the diagnosis, differential diagnosis, and disease severity assessment in patients with PSP. Our findings should be viewed as hypothesis generating, and further research is needed to replicate these results in a larger sample. ■

Acknowledgments: We thank all the patients and family members who participated in the study. We are grateful to APRINOIA Therapeutics for the provision of the ¹⁸F-APN-1607 precursor.

Data Availability Statement

Data available on request from the authors. ■

References

1. Rösler TW, Tayanian Marvian A, Brendel M, et al. Four-repeat tauopathies. *Prog Neurobiol* 2019;180:101644.
2. Boxer AL, Yu JT, Golbe LI, Litvan I, Lang AE, Höglinger GU. Advances in progressive supranuclear palsy: new diagnostic criteria, biomarkers, and therapeutic approaches. *Lancet Neurol* 2017;16(7):552–563.
3. Höglinger GU, Respondek G, Stamelou M, et al. Clinical diagnosis of progressive supranuclear palsy: the movement disorder society criteria. *Mov Disord* 2017;32:853–864.
4. Schonhaut DR, McMillan CT, Spina S, et al. 18F-flortaucipir tau positron emission tomography distinguishes established progressive supranuclear palsy from controls and Parkinson disease: a multicenter study. *Ann Neurol* 2017;82:622–634.
5. Passamonti L, Vázquez Rodríguez P, Hong YT, et al. 18F-AV-1451 positron emission tomography in Alzheimer’s disease and progressive supranuclear palsy. *Brain* 2017;140:781–791.
6. Hsiao IT, Lin KJ, Huang KL, et al. Biodistribution and radiation dosimetry for the tau tracer 18F-THK-5351 in healthy human subjects. *J Nucl Med* 2017;58(9):1498–1503.
7. Brendel M, Schönecker S, Höglinger G, et al. [18F]-THK5351 PET correlates with topology and symptom severity in progressive supranuclear palsy. *Front Aging Neurosci* 2018;9:440. <https://doi.org/10.3389/fnagi.2017.00440>.
8. Endo H, Shimada H, Sahara N, et al. In vivo binding of a tau imaging probe, [¹¹C]PBB3, in patients with progressive supranuclear palsy. *Mov Disord* 2019;34(5):744–754.
9. Perez-Soriano A, Arena JE, Dinelle K, et al. PBB3 imaging in parkinsonian disorders: Evidence for binding to tau and other proteins. *Mov Disord* 2017;32(7):1016–1024.
10. Ni R, Ji B, Ono M, et al. Comparative in vitro and in vivo quantifications of pathologic tau deposits and their association with neurodegeneration in tauopathy mouse models. *J Nucl Med* 2018;59(6):960–966.
11. Brendel M, Barthel H, van Eimeren T, et al. Assessment of 18 F-PI-2620 as a biomarker in progressive supranuclear palsy. *JAMA Neurol* 2020;77:1408–1419.

12. Tagai K, Ono M, Kubota M, et al. High-contrast in vivo imaging of tau pathologies in Alzheimer's and non-Alzheimer's disease tauopathies. *Neuron* 2021;109(1):42–58.
13. Hsu JL, Lin KJ, Hsiao IT, et al. The imaging features and clinical associations of a novel tau PET tracer–18F-APN1607 in Alzheimer's disease. 2020;45(10):747–756.
14. Postuma RB, Berg D, Stern M, et al. MDS clinical diagnostic criteria for Parkinson's disease. *Mov Disord* 2015;30(12):1591–1601.
15. Gilman S, Wenning GK, Low PA, et al. Second consensus statement on the diagnosis of multiple system atrophy background: a consensus conference on multiple system atrophy (MSA) in 1998 established. *Neurology* 2008;71(9):670–676.
16. Goetz CG, Tilley BC, Shaftman SR, et al. Movement Disorder Society-sponsored revision of the unified Parkinson's disease rating scale (MDS-UPDRS): scale presentation and clinimetric testing results. *Mov Disord* 2008;23(15):2129–2170.
17. Golbe LI, Ohman-Strickland PA. A clinical rating scale for progressive supranuclear palsy. *Brain* 2007;130(Pt6):1552–1565.
18. Lu J, Bao W, Li M, et al. Associations of [18F]-APN-1607 tau PET binding in the brain of Alzheimer's disease patients with cognition and glucose metabolism. *Front Neurosci* 2020;14:603. <https://doi.org/10.3389/fnins.2020.00604>.
19. Maldjian JA, Laurienti PJ, Kraft RA, Burdette JH. An automated method for neuroanatomic and cytoarchitectonic atlas-based interrogation of fMRI data sets. *Neuroimage* 2003;19(3):1233–1239.
20. Kovacs GG, Lukic MJ, Irwin DJ, et al. Distribution patterns of tau pathology in progressive supranuclear palsy. *Acta Neuropathol* 2020;140(2):99–119.
21. YODEN WJ. Index for rating diagnostic tests. *Cancer* 1950;3(1):32–35.
22. Kovacs GG, Xie SX, Robinson JL, et al. Sequential stages and distribution patterns of aging-related tau astroglial pathology (ARTAG) in the human brain. *Acta Neuropathol Commun* 2018;6(1):50.
23. Okamura N, Harada R, Ishiki A, Kikuchi A, Nakamura T, Kudo Y. The development and validation of tau PET tracers: current status and future directions. *Clin Transl Imaging* 2018;6(4):305–316.
24. Perez-Soriano A, Stoessl AJ. Tau imaging in progressive supranuclear palsy. *Mov Disord* 2017;32:91–93.
25. Ng KP, Pascoal TA, Mathoraarachchi S, et al. Monoamine oxidase B inhibitor, selegiline, reduces 18F-THK5351 uptake in the human brain. *Alzheimers Res Ther* 2017;9:25.
26. Marquié M, Normandin MD, Vandenberg CR, et al. Validating novel tau positron emission tomography tracer [F-18]-AV-1451 (T807) on postmortem brain tissue. *Ann Neurol* 2015;78(5):787–800.
27. Cho H, Choi JY, Lee SH, Ryu YH, Lee MS, Lyoo CH. 18F-AV-1451 binds to putamen in multiple system atrophy. *Mov Disord* 2017;32(1):171–173.
28. Nicastro N, Rodriguez PV, Malpetti M, et al. 18F-AV1451 PET imaging and multimodal MRI changes in progressive supranuclear palsy. *J Neurol* 2020;267(2):341–349.
29. Schweighauser M, Shi Y, Tarutani A, et al. Structures of α -synuclein filaments from multiple system atrophy. *Nature* 2020;585(7825):464–469.
30. Dickson DW, Ahmed Z, Algom AA, Tsuboi Y, Josephs KA. Neuropathology of variants of progressive supranuclear palsy. *Curr Opin Neurol* 2010;23(4):394–400.

Supporting Data

Additional Supporting Information may be found in the online version of this article at the publisher's web-site.

SGML and CITI Use Only
DO NOT PRINT

Author Roles

(1) Research project: A. Conception, B. Organization, C. Execution; (2) Statistical Analysis: A. Design, B. Execution, C. Review and Critique; (3) Manuscript: A. Writing of the first draft, B. Review and Critique. L.L.: 1A, 1B, 1C, 2A, 2B, 2C, 3A, 3B.

F.-T.L.: 1A, 1B, 1C, 2A, 2B, 2C, 3A, 3B.

M.L.: 1A, 1B, 1C, 2A, 2B, 2C, 3A, 3B.

J.-Y.L.: 1A, 1B, 1C, 2A, 2C, 3B.

Y.-M.S.: 1A, 1B, 1C,, 2A, 2C, 3B.

W.B.: 1A, 1B, 1C,, 2A, 2C, 3B.

Q.-S.C.: 1A, 1B, 1C,, 2A, 2C, 3B.

X.-Y.L.: 1A, 1B, 1C,, 2A, 2C, 3B.

X.-Y.Z.: 1A, 1B, 1C, 2A, 2C, 3B.

Y.G.: 1A, 1B, 1C, 2C, 3B.

J.-J.W.: 1A, 1B, 1C, 2C, 3B.

T.-C.Y.: 1A, 1B, 1C, 2C, 3B.

M.-K.J.: 1A, 1B, 1C, 2C, 3B.

J.W.: 1A, 1B, 1C, 2C, 3B.

C.Z.: 1A, 1B, 1C, 2C, 3B.

X.L.: 2B, 2C.

J.-F.L.: 2C, 3B.

Financial Disclosures

The content of this article represents original work that has not been previously published and is not under consideration for publication elsewhere.

Tzu-Chen Yen and Ming-Kuei Jang are employees of APRINOIA Therapeutics Co. (Suzhou, China).